

Fluid photonic crystal from colloidal quantum dots

V. N. Mantsevich^{1,*} and S. A. Tarasenko²¹*Moscow State University, 119991, Moscow, Russia*²*Ioffe Institute, 194021, St. Petersburg, Russia*

(Received 4 May 2017; published 29 September 2017)

We study optical forces acting upon semiconductor quantum dots and the force-driven motion of the dots in a colloid. In the spectral range of exciton transitions in quantum dots, when the photon energy is close to the exciton energy, the polarizability of the dots is drastically increased. It leads to a resonant increase of both the gradient and the scattering contributions to the optical force, which enables the efficient manipulation with the dots. We reveal that the optical grating of the colloid leads to the formation of a fluid photonic crystal with spatially periodic circulating fluxes and density of the dots. Pronounced resonant dielectric response of semiconductor quantum dots enables a separation of the quantum dots with different exciton frequencies.

DOI: [10.1103/PhysRevA.96.033855](https://doi.org/10.1103/PhysRevA.96.033855)

I. INTRODUCTION

Optical fields interacting with micro- and nanoparticles induce sizable mechanical forces acting upon the particles, which enables their trapping and precise manipulation [1,2]. Such noninvasive optomechanical approaches have been demonstrated for dielectric [3–5], metallic [6–9], semiconductor [10–12] particles, as well as biological cells [13–15]. Using photonic interference schemes, one can create the arrays of optical traps and form the lattices of dielectric particles [16] or biomolecules [17]. Among other achievements of optomechanics are measurements of interaction forces between molecules [18] and optical forces with femtonewton resolution [19].

Highly interesting objects for optical trapping and manipulation are colloidal nanocrystals (or quantum dots, QDs) [10–12], since they are important for sensor and biological applications, particularly as superior fluorescent labels [20–23]. The optical force acting upon a QD is determined by the dot polarizability [24], which has a resonant behavior at the frequency of exciton transitions in the QD, when the radiation excites electron-hole pairs (excitons) in the dot [25,26]. Far from the exciton resonance, the polarizability is given by the background dielectric contrast between the QD material and the environment and commonly described by the Clausius-Mossotti relation. Optical trapping of colloidal CdTe- and CdSe-core QDs in such conditions has been demonstrated in Refs. [10–12]. Close to the exciton resonance, the QD polarizability and, correspondingly, the optical force are drastically enhanced. Currently, there is a lack of theoretical studies of this effect as well as the optical-force-driven dynamics of quantum dots in the colloid.

Here, we study the optical force acting upon a QD and the force-driven fluxes of QDs in a colloid induced by optical grating. We consider that the dielectric response of a QD is caused by exciton transitions and has a resonant behavior. The force can be split in two contributions: the gradient force and the scattering-absorption force determined by the real and imaginary parts of the susceptibility, respectively [24,27]. Close to the excitonic resonance, both contributions increase

and are comparable to each other. In the presence of both contributions, the total force is nonconservative and cannot be described by a potential. Therefore, the optical grating of a colloid leads to the formation of spatially periodic density of the dots as well as the emergence of spatially periodic circulating fluxes of the dots (Brownian vertexes [28]). The emerging modulation of the QD density and fluxes results, in turn, in the periodic modulation of the optical properties of the colloid, such as the refractive index. As a result, the system demonstrates the properties of a photonic crystal. By considering the interplay of optical forces and the processes of viscous friction and diffusion of dots, we study the occurrence of such a fluid photonic crystal from colloidal dots. We calculate the steady-state distributions of the dot density and fluxes as well as the time scales of the photon crystal formation.

II. THEORY

A. Optical force acting upon a quantum dot

We consider a cell with a colloidal solution of semiconductor QDs excited by two coherent laser beams of the *s* polarization and the same frequency ω , as shown in Fig. 1. The laser fields interfere and produce an optical grating. The total electric field of the radiation in the solution is given by $\mathcal{E}(\mathbf{r}, t) = \text{Re}[\mathbf{E}(\mathbf{r})e^{-i\omega t}]$, where

$$\mathbf{E}(\mathbf{r}) = (E_1 e^{i\mathbf{q}_1 \cdot \mathbf{r}} + E_2 e^{i\mathbf{q}_2 \cdot \mathbf{r}}) \hat{\mathbf{y}}, \quad (1)$$

E_1 and E_2 are the (real) amplitudes of the laser electric fields in the solution, which are determined by the amplitudes of the incident fields, E_{10} and E_{20} , respectively, and the Fresnel transmission coefficient; $\mathbf{q}_1 = q(\sin\theta, 0, \cos\theta)$ and $\mathbf{q}_2 = q(-\sin\theta, 0, \cos\theta)$ are the wave vectors, where $q = \omega n_\omega / c$ and θ is the angle of refraction, which is related to the angle of incidence θ_0 by Snell's law $\sin\theta_0 = n_\omega \sin\theta$; n_ω is the refractive index of the solution; c is the speed of light; and $\hat{\mathbf{y}}$ is the unit vector along the *y* axis. The intensity of the radiation I for the geometry we consider depends on the *x* axis only and is given by

$$I = \frac{cn_\omega}{8\pi} |\mathbf{E}|^2 = \frac{cn_\omega}{8\pi} [E_1^2 + E_2^2 + 2E_1 E_2 \cos(2xq \sin\theta)]. \quad (2)$$

*vmantsev@gmail.com

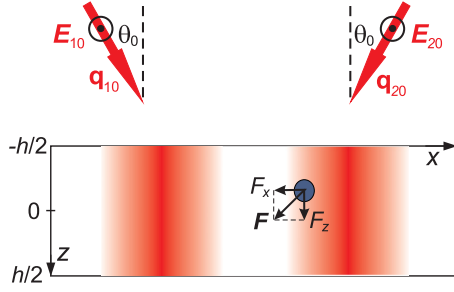


FIG. 1. Optical grating in a colloidal solution of quantum dots induced by two coherent laser beams leads to the emergence of a position-dependent optical force acting upon quantum dots. Color intensity illustrates the distribution of radiation intensity in the cell with the colloid; h is the depth of the cell.

The radiation interacts with a QD and produces a force acting upon the dot. For the case of small QDs compared to the light wavelength (typical QD sizes are a few nm while the light wavelength in a colloid is few hundred of nm), the projections of the optical force acting upon the dot located at the \mathbf{r} point are given by [2,24]

$$F_j(\omega) = \frac{1}{2} \sum_{j'} \text{Re} \left[\alpha E_{j'}(\mathbf{r}) \frac{\partial E_{j'}^*(\mathbf{r})}{\partial r_j} \right], \quad (3)$$

where j and j' run over the Cartesian coordinates x , y , and z ; $E_j(\mathbf{r})$ is the j projection of the electric field in the colloid $\mathbf{E}(\mathbf{r})$ given by Eq. (1); and α is the QD polarizability. The optical force is proportional to the QD polarizability and scales quadratically with the electric field. This is because the force originates from the interaction of the oscillating electric dipole moment of the QD, induced in turn by the ac electric field and determined by the dot polarizability, with the ac electric field. In the regime of weak light-matter coupling, which we consider, for the electric field in Eq. (3) it is sufficient to use the unperturbed field of the laser beams (1). We note, however, that the optical force requires more sophisticated self-consistent calculations if the particle itself considerably affects the electric field distribution as can happen, e.g., in the case of strong light confinement [29–32].

The dielectric response of the QD caused by exciton transitions within the dot has a resonant behavior and the polarizability has the form [26]

$$\alpha(\omega, q) = \frac{\pi a_B^3 \omega_{LT}}{\omega_0 - \omega - i(\Gamma + q^3 a_B^3 \omega_{LT}/6)}, \quad (4)$$

where ω_0 is the resonance frequency corresponding to the exciton transitions, a_B is the Bohr radius of the exciton, ω_{LT} is the frequency corresponding to the longitudinal-transverse splitting of exciton states in the host semiconductor of the QD, which determines the strength of light-matter coupling in semiconductors at interband optical transitions. The radiative decay rate of excitons is described by the term $q^3 a_B^3 \omega_{LT}/6$, the parameter Γ stands for the nonradiative decay rate of excitons. The background dielectric contrast of the QD material and the liquid substance is neglected.

Straightforward calculations show that the optical force has two contributions: $\mathbf{F} = \mathbf{F}^{(\text{gr})} + \mathbf{F}^{(\text{sc})}$. The first (gradient)

contribution $\mathbf{F}^{(\text{gr})}$ is determined by the real part of the QD polarizability. Substitution of Eq. (1) for the electric field in Eq. (3) yields

$$F_x^{(\text{gr})} = -q \sin \theta (\text{Re} \alpha) E_1 E_2 \sin(2xq \sin \theta). \quad (5)$$

Taking into account Eq. (4) for the QD polarizability and Eq. (2) for the intensity of radiation, we obtain

$$F_x^{(\text{gr})} = \frac{2\pi^2}{cn_\omega} \frac{a_B^3 \omega_{LT}(\omega_0 - \omega)}{(\omega_0 - \omega)^2 + (\Gamma + q^3 a_B^3 \omega_{LT}/6)^2} \frac{dI}{dx}. \quad (6)$$

This contribution to the optical force is directed along or opposite to the light intensity gradient depending on the detuning between the laser field frequency and the exciton frequency.

The second contribution $\mathbf{F}^{(\text{sc})}$, commonly referred to as the scattering and absorbing force, is determined by the imaginary part of the QD polarizability and has nonzero x and z projections. They can be obtained by the substitution of Eqs. (1) and (4) in Eq. (3), which yields

$$\begin{aligned} F_x^{(\text{sc})} &= \frac{q \sin \theta}{2} (\text{Im} \alpha) [E_1^2 - E_2^2] \\ &= \frac{q \sin \theta}{2} \frac{\pi a_B^3 \omega_{LT} (\Gamma + q^3 a_B^3 \omega_{LT}/6)}{(\omega_0 - \omega)^2 + (\Gamma + q^3 a_B^3 \omega_{LT}/6)^2} [E_1^2 - E_2^2], \end{aligned} \quad (7)$$

$$\begin{aligned} F_z^{(\text{sc})} &= \frac{q \cos \theta}{2} (\text{Im} \alpha) [E_1^2 + E_2^2 + 2E_1 E_2 \cos(2xq \sin \theta)] \\ &= \frac{4\pi^2 q \cos \theta}{cn_\omega} \frac{a_B^3 \omega_{LT} (\Gamma + q^3 a_B^3 \omega_{LT}/6)}{(\omega_0 - \omega)^2 + (\Gamma + q^3 a_B^3 \omega_{LT}/6)^2} I. \end{aligned} \quad (8)$$

The scattering contribution to the total optical force reaches a maximum at the frequency of the exciton resonance.

We consider in what follows that the amplitudes of the incident laser beams are equal to each other, i.e., $E_1 = E_2$. In this case, $F_x^{(\text{sc})}$ vanishes and the scattering force points along the line of the equal intensity of radiation. The total force can be presented in the form

$$\mathbf{F} = F_{0x} \sin(kx) \hat{\mathbf{x}} + F_{0z} [1 + \cos(kx)] \hat{\mathbf{z}}, \quad (9)$$

where

$$\begin{aligned} F_{0x} &= -\frac{4\pi^2}{cn_\omega} \frac{a_B^3 \omega_{LT}(\omega_0 - \omega) q \sin \theta}{(\omega_0 - \omega)^2 + (\Gamma + q^3 a_B^3 \omega_{LT}/6)^2} I_0, \\ F_{0z} &= \frac{4\pi^2}{cn_\omega} \frac{a_B^3 \omega_{LT} (\Gamma + q^3 a_B^3 \omega_{LT}/6) q \cos \theta}{(\omega_0 - \omega)^2 + (\Gamma + q^3 a_B^3 \omega_{LT}/6)^2} I_0, \end{aligned} \quad (10)$$

$k = 2q \sin \theta$, and $I_0 = (cn_\omega/4\pi)E_1^2$. For the parameters $\hbar\omega_0 = 2.35$ eV, $a_B^3 \omega_{LT} = 0.25 \times 10^{-6}$ cm³/s [26], $\hbar\Gamma = 30$ μ eV [34], and $q^3 a_B^3 \omega_{LT}/6 \ll \Gamma$ corresponding to CdSe quantum dots, the optical force F_0 can be estimated as 0.1 fN for the radiation intensity $I_0 = 1$ kW/cm².

B. Circulating currents and separation of dots

In the presence of the scattering contribution, the total optical force is nonconservative (does not conserve mechanical

energy) and cannot be described as a gradient of the light-induced potential. Mathematically, it follows from the fact that $\nabla \times \mathbf{F} \neq 0$ for the force \mathbf{F} given by Eq. (9) and the net work done by the optical force in moving a dot around a closed loop is nonzero. Therefore, the optical grating of a colloidal solution leads not only to the formation of spatially periodic density of the dots but also to the emergence of spatially periodic circulating fluxes of the dots. The emergence of a Brownian vortex of a similar nature in a single-beam optical tweezer has been demonstrated in Ref. [28]. The one-dimensional motion of dielectric particles in an viscous medium in an optical waveguide was considered in Ref. [32].

The kinetics of quantum dots in the solution is governed by the interplay of the optical forces and the forces of viscous friction as well as the processes of dot diffusion. The local concentration of the dots $n(x, z, t)$ and the dot flux $\mathbf{j}(x, z, t)$ are related by the continuity equation

$$\frac{\partial n}{\partial t} + \nabla \cdot \mathbf{j} = 0. \quad (11)$$

The dots flux consists of the drift and diffusion terms,

$$\mathbf{j} = \mathbf{j}^{(\text{drift})} + \mathbf{j}^{(\text{diff})}. \quad (12)$$

The drift term is proportional to the optical force driving the dots and given by

$$\mathbf{j}^{(\text{drift})} = \mu n \mathbf{F}, \quad (13)$$

where μ is the mobility of dots in the solution. The diffusion term is determined by the spatial inhomogeneity of the dot concentration and has the form

$$\mathbf{j}^{(\text{diff})} = -D \nabla n, \quad (14)$$

where D is the diffusion coefficient. In thermal equilibrium, the mobility and the diffusion coefficient are connected with each other by the Einstein relation $D = \mu k_B T$, where k_B is the Boltzmann constant and T is the temperature. The diffusion coefficient of quantum dots with radii 15–20 nm in the glycerol-water solutions with the viscosity 45–55 cP at room temperature was experimentally determined to be 0.5–0.7 $\mu\text{m}^2/\text{s}$ [33]. These experimental values were found to be in a good agreement with the Stokes-Einstein relation for the diffusion coefficient of spherical particles in a liquid with a low Reynolds number.

To solve the equation set (11)–(14), we present the local concentration of the dots as the sum $n = n_0 + \delta n$, with n_0 being the average concentration and δn being the correction. Then, in the regime linear in the light intensity, Eqs. (11)–(14) yield

$$\frac{\partial \delta n}{\partial t} - D \Delta \delta n = -\mu n_0 \nabla \cdot \mathbf{F} \quad (15)$$

and

$$\mathbf{j} = \mu n_0 \mathbf{F} - D \nabla \delta n. \quad (16)$$

Equations (15) and (16) are to be solved with boundary conditions. We consider the boundary conditions of zero fluxes through the cell bottom and top, i.e.,

$$j_z|_{z=\pm h/2} = 0, \quad (17)$$

where h is the cell depth.

For the particular form of the optical force given by Eq. (9), the solution of the diffusion Eq. (15) can be presented in the form

$$\delta n(x, z, t) = a(z, t) + b(z, t) \cos(kx). \quad (18)$$

This decomposition leads to the equations

$$\frac{\partial a}{\partial t} - D \frac{d^2 a}{dz^2} = 0, \quad \frac{\partial b}{\partial t} - D \left(\frac{d^2 b}{dz^2} - k^2 b \right) = -\mu n_0 F_{0x} k, \quad (19)$$

and the boundary conditions

$$\left. \frac{da}{dz} \right|_{z=\pm h/2} = \frac{n_0 F_{0z}}{k_B T}, \quad \left. \frac{db}{dz} \right|_{z=\pm h/2} = \frac{n_0 F_{0z}}{k_B T}, \quad (20)$$

where we took into account the relation $D = \mu k_B T$.

Equations (19) with the boundary conditions (20) and an arbitrary initial distribution of quantum dots in the solution can be solved by the Laplace transform method. We assume that the solution was initially in thermal equilibrium and then, at $t = 0$, the laser radiation is switched on. In this case, the functions $a(z, t)$ and $b(z, t)$ at $t \geq 0$ are given

$$\begin{aligned} a(z, t) &= \frac{n_0 F_{0z}}{k_B T} \left[z - \frac{4}{h} \sum_{n=0}^{\infty} \frac{(-1)^n \sin k_n z}{k_n^2} e^{-D k_n^2 t} \right], \\ b(z, t) &= -\frac{n_0 F_{0x}}{k_B T k} [1 - e^{-D k^2 t}] + \frac{n_0 F_{0z}}{k_B T k} \left[\frac{\sinh kz}{\cosh(kh/2)} \right. \\ &\quad \left. - \frac{4}{h} \sum_{n=0}^{\infty} \frac{(-1)^n \sin k_n z}{k^2 + k_n^2} e^{-D(k^2 + k_n^2)t} \right], \end{aligned} \quad (21)$$

where $k_n = (\pi/h)(1 + 2n)$. The maps of the dot concentration $\delta n(x, z, t)$ and the dot fluxes $\mathbf{j}(x, z, t)$ can be readily found from Eqs. (18) and (16), respectively.

The steady-state distributions of the dot concentration and the dot fluxes induced by cw radiation can be obtained by considering the limit of the functions $a(z, t)$ and $b(z, t)$ at $t \rightarrow \infty$. This yields

$$\delta n = \frac{n_0 F_{0z}}{k_B T} z + \frac{n_0}{k_B T} \left[F_{0z} \frac{\sinh(kz)}{\cosh(kh/2)} - F_{0x} \right] \frac{\cos kx}{k} \quad (22)$$

and

$$\begin{aligned} j_x &= \mu n_0 F_{0z} \frac{\sinh(kz)}{\cosh(kh/2)} \sin(kx), \\ j_z &= \mu n_0 F_{0z} \left[1 - \frac{\cosh(kz)}{\cosh(kh/2)} \right] \cos(kx). \end{aligned} \quad (23)$$

The steady-state spatial modulation of dot concentration is produced by both F_x and F_z components of the optical force while the steady-state fluxes are induced by the nonconservative F_z component only.

III. RESULTS AND DISCUSSION

Figure 2 demonstrates the steady-state maps of the quantum dot density $n(x, z)$ and the dot circulating fluxes $\mathbf{j}(x, z)$ induced by the optical grating of a colloidal solution. The density distribution $n(x, z)$ is encoded by color and the flux distribution $\mathbf{j}(x, z)$ is shown by black arrows. Figures 2(a), 2(b) and 2(c) correspond to a negative, zero, and a positive detuning $\omega_0 - \omega$

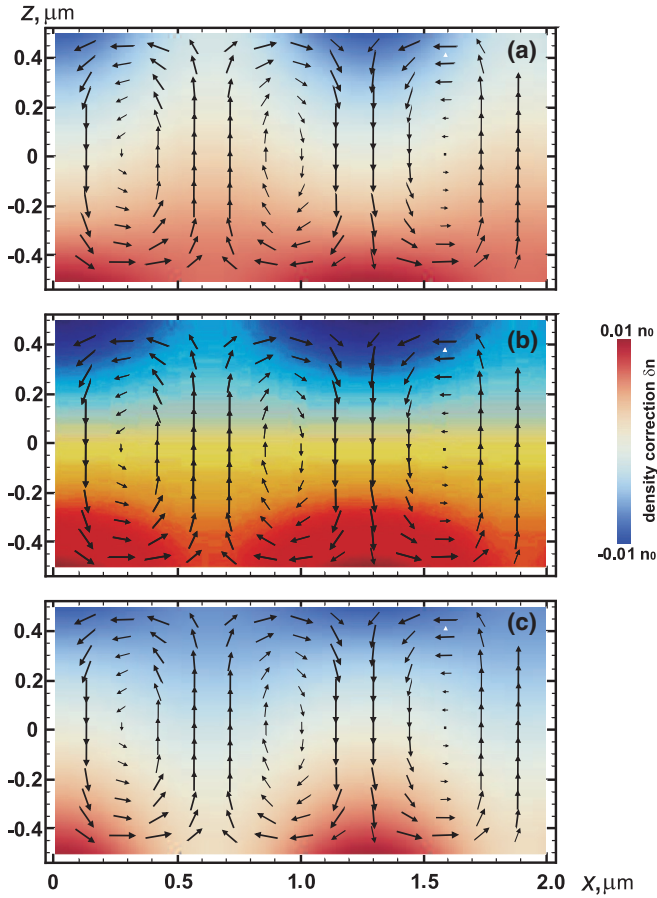


FIG. 2. Steady-state distributions of the dot density (color map) and the dot circulating fluxes (arrows) in a colloidal solution induced by optical grating, as sketched in Fig. 1. Panels (a), (b), and (c) correspond to the negative detuning $\omega_0 - \omega = -3\Gamma$, zero detuning $\omega_0 = \omega$, and positive detuning $\omega_0 - \omega = 3\Gamma$, respectively. All the distributions are calculated after Eqs. (22) and (23) for the parameters $\hbar\omega_0 = 2.35$ eV, $\hbar\Gamma = 30$ μ eV [34], and $a_B^3\omega_{LT} = 0.25 \times 10^{-6}$ cm³/s [26] corresponding to CdSe quantum dots, $T = 300$ K, $k = 0.5 \times 10^5$ cm⁻¹, $\theta = 8^\circ$, $h = 1$ μ m, and $I_0 = 1$ kW/cm².

between the dot resonant frequency ω_0 and the radiation frequency ω . Typically, the resonant frequencies of the dots in a solution have a dispersion due to, e.g., the dispersion of the dot sizes. The optical grating leads to the formation of a spatially periodic density of the dots in the longitudinal direction x and inhomogeneous distribution of the dots in the vertical direction z . The modulation $\delta n/n_0$ is about 1% for the radiation intensity 1 kW/cm². At fixed temperature and radiation intensity, the modulation of the QD density is determined by the frequency detuning $\omega_0 - \omega$, the radiative and nonradiative decay rates of excitons, Γ , and $q^3 a_B^3 \omega_{LT}/6$, respectively. The nonradiative decay rate is typically much larger than the radiative decay rate at room temperature. Therefore, the higher degree of the QD density modulation and the higher spectral sensitivity of the QDs are expected for QDs with suppressed nonradiative channels of exciton recombination.

Quantum dots with the exciton frequencies detuned from the radiation frequency [Figs. 2(a) and 2(c)] are acted upon

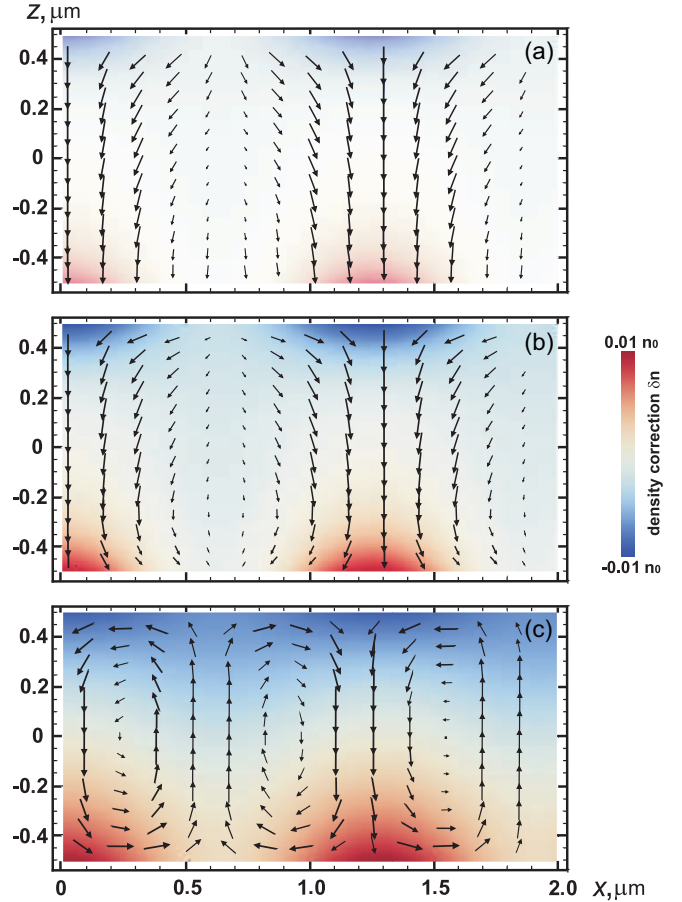


FIG. 3. Snapshots of the distributions of the dot density (color map) and the dot fluxes (arrows) at the times (a) $t = 0.002$ s, (b) $t = 0.02$ s, and (c) $t = 0.1$ s after the radiation is switched on. The distribution are calculated for the parameters of Fig. 2(c) and the diffusion coefficient $D = 0.5 \times 10^{-8}$ cm²/s.

by both the scattering component F_z and the gradient component F_x of the optical force. The scattering component is directed along the z axis but its magnitude depends on the longitudinal coordinate x ; see Eq. (10). It leads to the formation of a vertical profile of the dot density and a spatially periodic dot density in the longitudinal direction at the cell top and bottom. More important, the scattering force gives rise to persistent circulating fluxes of the dots shown by black arrows. The circulating fluxes are more pronounced in cells with the depth h comparable to and exceeding the wavelength $2\pi/k$ since in shallower cells the vertical motion of the dots is suppressed. The gradient component F_x leads to the formation of a spatially periodic density of the dots in the longitudinal direction. This effect is most clearly visible at $z = 0$. The direction of the gradient force depends on the sign of the detuning; therefore the density modulation at $z = 0$ is of opposite signs for the dots with positive [Fig. 2(a)] and negative [Fig. 2(c)] detuning.

For quantum dots with the resonant frequency corresponding to the radiation frequency [Fig. 2(b)], the gradient component F_x vanishes and the kinetics is solely determined by the scattering force F_z . The scattering force gives rise to the inhomogeneous distribution of the dots as well as the circulating fluxes of the dots.

Figure 3 shows some stages of the steady-state distribution formation after the laser radiation is switched on. As follows from Eqs. (21), the time scale of the formation of longitudinal periodic density of the dots is determined by the time $\tau = 1/(Dk^2)$. For the wave vector $k = 0.5 \times 10^4 \text{ cm}^{-2}$ and the diffusion coefficient $D = 0.5 \times 10^{-8} \text{ cm}^2/\text{s}$, this time $\tau \approx 0.1 \text{ s}$. Figures 3(a), 3(b), and 3(c) show the snapshots of the density and flux distributions at $t = 0.002, 0.02, \text{ and } 0.1 \text{ s}$, respectively. Just after the radiation is switched on, the dots are homogeneously distributed in the solution. At this stage, the dot fluxes are completely determined by optical forces since there are no contributions related to the dot density gradients. At large times, the density gradients are formed, the fluxes become closed, and the distributions approach the steady-state ones.

IV. SUMMARY

We have presented a theoretical study of optical forces acting on semiconductor quantum dots in a colloid and

formation of a fluid photonic crystal from the dots by optical grating. In such a system, the density of the dots and the fluxes of the dots are periodically modulated in space, suggesting the periodic modulation of the optical properties of the colloid. By considering the interplay of the optical forces and the processes of viscous friction and diffusion of dots, we have calculated the steady-state distributions of the dot density and fluxes as well as the time scales of the fluid photonic crystal formation. The results can be employed for creating dynamic photonic structures with tunable parameters and further study of their optical properties. Other possible applications include optically induced mixing of colloids and the separation of quantum dots with different resonant frequencies.

ACKNOWLEDGMENTS

This work was supported by RF President Grant for Young Scientists No. MD-4550.2016.2 and RFBR Grant No. 16-02-00204.

-
- [1] A. Ashkin, Acceleration and Trapping of Particles by Radiation Pressure, *Phys. Rev. Lett.* **24**, 156 (1970).
 - [2] A. Ashkin and J. M. Dziedzic, Optical levitation of liquid drops by radiation pressure, *Science* **187**, 1073 (1975).
 - [3] M. M. Burns, J. M. Fournier, and J. A. Golovchenko, Optical Matter: Crystallization and binding in intense optical fields, *Science* **249**, 749 (1990).
 - [4] T. Čížmár, M. Šiler, M. Šerý, P. Zemánek, V. Garcés-Chávez, and K. Dholakia, Optical sorting and detection of submicrometer objects in a motional standing wave, *Phys. Rev. B* **74**, 035105 (2006).
 - [5] A. H. J. Yang, S. D. Moore, B. S. Schmidt, M. Klug, M. Lipson, and D. Erikson, Optical manipulation of nanoparticles and biomolecules in sub-wavelength slot waveguides, *Nature (London)* **457**, 71 (2009).
 - [6] K. Svoboda and S. M. Block, Optical trapping of metallic Rayleigh particles, *Opt. Lett.* **19**, 930 (1994).
 - [7] P. M. Hansen, V. K. Bhatia, N. Harrit, and L. Oddershede, Expanding the optical trapping range of gold nanoparticles, *Nano Lett.* **5**, 1937 (2005).
 - [8] N. Huang, L. J. Martinez, F. Jaquay, A. Nakano, and M. L. Povinelli, Ultrastrong optical binding of metallic nanoparticles, *Nano Lett.* **15**, 5841 (2015).
 - [9] M. I. Petrov, S. V. Sukhov, A. A. Bogdanov, A. S. Shalin, and A. Dogariu, Surface plasmon polariton assisted optical pulling force, *Laser Photon. Rev.* **10**, 116 (2016).
 - [10] L. Pan, A. Ishikawa, and N. Tamai, Detection of optical trapping of CdTe quantum dots by two-photon-induced luminescence, *Phys. Rev. B* **75**, 161305 (2007).
 - [11] L. Jauffred, A. C. Richardson, and L. B. Oddershede, Three-dimensional optical control of individual quantum dots, *Nano Lett.* **8**, 3376 (2008).
 - [12] L. Jauffred and L. B. Oddershede, Two-photon quantum dot excitation during optical trapping, *Nano Lett.* **10**, 1927 (2010).
 - [13] A. Ashkin, J. M. Dziedzic, and T. Yamane, Optical trapping and manipulation of single cells using infrared laser beams, *Nature (London)* **330**, 769 (1987).
 - [14] X. Wang, S. Chen, M. Kong, Z. Wang, K. D. Costa, R. A. Li, and D. Sun, Enhanced cell sorting and manipulation with combined optical tweezer and microfluidic chip technologies, *Lab Chip* **11**, 3656 (2011).
 - [15] M.-C. Zhong, X.-B. Wei, J.-H. Zhou, Z.-Q. Wang, and Y.-M. Li, Trapping red blood cells in living animals using optical tweezers, *Nat. Commun.* **4**, 1768 (2013).
 - [16] A. N. Grigorenko, N. W. Roberts, M. R. Dickson, and Y. Zhang, Nanometric optical tweezers based on nanostructured substrates, *Nat. Photon.* **2**, 365 (2008).
 - [17] M. Soltani, J. Lin, R. A. Forties, J. T. Inman, S. N. Saraf, R. M. Fulbright, M. Lipson, and M. D. Wang, Nanophotonic trapping for precise manipulation of biomolecular arrays, *Nat. Nanotechnol.* **9**, 448 (2014).
 - [18] J. C. Meiners and S. R. Quake, Femtonewton Force Spectroscopy of Single Extended DNA Molecules, *Phys. Rev. Lett.* **84**, 5014 (2000).
 - [19] C. Zensen, N. Villadsen, F. Winterer, S. R. Keiding, and T. Lohmuller, Pushing nanoparticles with light: A femtonewton resolved measurement of optical scattering forces, *APL Photon.* **1**, 026102 (2016).
 - [20] B. Dubertret, P. Scourides, D. J. Norris, V. Noireaux, A. H. Brivanlou, and A. Libchaber, In vivo imaging of quantum dots encapsulated in phospholipid micelles, *Science* **298**, 1759 (2002).
 - [21] M. Dahan, S. Levi, C. Luccardini, P. Rostaing, B. Riveau, and A. Triller, Diffusion dynamics of glycine receptors revealed by single-quantum dot tracking, *Science* **302**, 442 (2003).
 - [22] Y. Ebenstein, N. Gassman, S. Kim, J. Antelman, Y. Kim, S. Ho, R. Samuel, X. Michalet, and S. Weiss, Lighting up individual DNA binding proteins with quantum dots, *Nano Lett.* **9**, 1598 (2009).
 - [23] K. Yum, S. Na, Y. Xiang, N. Wang, and M. Yu, Mechanochemical delivery and dynamic tracking of fluorescent quantum dots in the cytoplasm and nucleus of living cells, *Nano Lett.* **9**, 2193 (2009).

- [24] P. C. Chaumet and M. Nieto-Vesperinas, Time-averaged total force on a dipolar sphere in an electromagnetic field, *Opt. Lett.* **25**, 1065 (2000).
- [25] F. Wang, J. Shan, M. A. Islam, I. P. Herman, M. Bonn, and T. F. Heinz, Exciton polarizability in semiconductor nanocrystals, *Nat. Mater.* **5**, 861 (2006).
- [26] E. L. Ivchenko, *Optical Spectroscopy of Semiconductor Nanostructures* (Alpha Science, Harrow, UK, 2005).
- [27] A. Rohrbach and E. H. K. Stelzer, Optical trapping of dielectric particles in arbitrary fields, *J. Opt. Soc. Am. A* **18**, 839 (2001).
- [28] B. Sun, J. Lin, E. Darby, A. Y. Grosberg, and D. G. Grier, Brownian vortices, *Phys. Rev. E* **80**, 010401 (2009).
- [29] M. L. Juan, R. Gordon, Y. Pang, F. Eftekhari, and R. Quidant, Self-induced back-action optical trapping of dielectric nanoparticles, *Nat. Phys.* **5**, 915 (2009).
- [30] J. T. Rubin and L. Deych, On optical forces in spherical whispering gallery mode resonators, *Opt. Express* **19**, 22337 (2011).
- [31] J. T. Rubin and L. Deych, Optical forces due to spherical microresonators and their manifestation in optically induced orbital motion of nanoparticles, *Phys. Rev. A* **84**, 023844 (2011).
- [32] A. F. Sadreev and E. Y. Sherman, Temporal oscillations of light transmission through dielectric microparticles subjected to optically induced motion, *Phys. Rev. A* **94**, 033820 (2016).
- [33] G. A. Lessard, P. M. Goodwin, and J. H. Werner, Three-dimensional tracking of individual quantum dots, *Appl. Phys. Lett.* **91**, 224106 (2007).
- [34] M. J. Fernée, P. Tamarat, and B. Lounis, Spectroscopy of single nanocrystals, *Chem. Soc. Rev.* **43**, 1311 (2014).